Dileptons from a chemically equilibrating quark-gluon plasma

Zejun He,[1,2,3] Jiali Long,[2] Weizhou Jiang,[2] Yugang Ma,[2] and Bo Liu[4]

[1]*CCAST (World Laboratory), P.O. Box 8730, Beijing 100080, China*
[2]*Shanghai Institute of Nuclear Research, Chinese Academy of Sciences, P.O. Box 800-204, Shanghai 201800, China*
[3]*Research Center of Nuclear Theory of National Laboratory of Heavy Ion Accelerator of Lanzhou, Lanzhou 730000, China*
[4]*Institute of High Energy Physics, Chinese Academy of Sciences, Beijing 100039, China*

We have studied the evolution and dilepton production of a chemically equilibrating quark-gluon system at finite baryon density. We found that due to the increase of the quark phase lifetime with increasing initial quark chemical potential and other factors, such as, higher initial temperature, larger gluon density, and gluon fusion or quark annihilation cross section, thermal charmed quarks provide a dominant contribution to the dilepton yield. This results in a significant enhancement of intermediate mass dilepton production.

I. INTRODUCTION

Lattice QCD results have indicated, hadronic matter probably undergoes a phase transition into a unconfined quark-gluon plasma (QGP) in ultrarelativistic nuclear collisions. The Relativistic Heavy-Ion Collider (RHIC) and the Large Hadron Collider will provide the best opportunity to study the formation and evolution of the QGP. Since the QGP exists only for a very short time (several fm) in a small volume (about 100 fm^3), a direct detection of this state of matter is not possible. Thus, various indirect signatures have to be used for its detection, such as the J/ψ suppression [1], strangeness enhancement [2], dilepton spectra, etc. [3–5]. Among many experimental observables, dileptons are considered to be the most promising because they do not suffer strong final interactions and are, therefore, expected to retain the information about the QGP.

Previously many authors [6–11], considering that the created QGP in collisions is a thermodynamic equilibrium system, have studied the dilepton production, and some of them have found that dileptons are suppressed with increasing initial quark chemical potential (and thus also initial baryon density). In recent years, Shuryak and co-workers [12,13] have indicated that due to large initial parton density of the QGP produced at the RHIC energies, the partons necessarily suffer many collisions in a very short time ($\tau \approx 0.3$–0.7 fm), thus, the system may attain kinetic equilibrium. However, in order to achieve chemical equilibrium, more quarks and antiquarks are needed, thus some energy is consumed, leading to the faster cooling of the system. Such a system may be away from the chemical equilibrium. In particular, taking into account transverse expansion, the large velocity gradient may drive the system further away from the chemical equilibrium [14]. One characterizes the nonequilibrium of the system by quark (antiquark) fugacity $\lambda_{q(\bar q)}$ and gluon fugacity λ_g which are less than unity. From master equations governing the evolution of parton densities and the equation of energy-momentum conservation of the QGP, Geiger and co-workers [15–18] have obtained a set of evolution equations of the chemically equilibrating baryon-free QGP system, and some of them have studied the effect of the chemical equilibration on the dilepton production in baryon-

free QGP. Hammon and co-workers [19,20] have calculated the initial conditions of the nonequilibrium QGP produced at the RHIC energies, from the perturbative QCD within the Glauber multiple scattering theory and indicated that the initial system has finite baryon density. Majunder and Gale [21] have also discussed about the dileptons from the QGP with finite baryon density, created at the RHIC energies. These show that one may further study the effect of the chemical equilibration on the dilepton production in a QGP with finite baryon density. As pointed out in Refs. [17,18,22–24], the distribution functions of partons in a chemically nonequilibrated system can be described by Jüttner distributions, $f_{q(\bar q)} = \lambda_{q(\bar q)}/(e^{(p \mp \mu_q)/T} + \lambda_{q(\bar q)})$ for quarks (antiquarks) and $f_g(p) = \lambda_g/(e^{p/T} - \lambda_g)$ for gluons. When the parton fugacities λ_i are much less than unity, as may happen during the early evolution of the parton system, the quantum effect may be neglected, the distributions are approximated as Boltzmann form $f_{q(\bar q)} = \lambda_{q(\bar q)} e^{-(p \mp \mu_q)/T}$ [25]. However, this introduces an error of the order of 40% when the distribution approaches chemical equilibrium as pointed out in Ref. [17]. It should be stressed here that the most commonly used approximations are the factorized Fermi-Dirac distribution functions, $f_{q(\bar q)} = \lambda_{q(\bar q)}/(e^{(p \mp \mu_q)/T} + 1)$ for quarks (antiquarks) and factorized Bose-Einstein distribution function $f_g(p) = \lambda_g/(e^{p/T} - 1)$ for gluons. As can be seen from the discussion in Ref. [17], the calculated thermal screening mass under this approximation coincides with that from the Jüttner distribution only near $\lambda_g = 1$, however, in the intermediate region of the λ_g the deviation is quite significant. It shows that it is difficult to study the whole process of the chemical equilibration of the system, and to obtain better results based on those previously approximated distribution functions of partons.

Previous authors mainly considered the dilepton production from the process $q\bar q \rightarrow l\bar l$ [3–5]. In recent years, possible sources of dileptons—such as, $q\bar q \rightarrow l\bar l$ annihilation, $qg \rightarrow ql\bar l$ the Compton-like scattering, and $qg \rightarrow qgl\bar l$ fusion—were investigated and at chemical and thermal equilibrium the spectrum was found to be dominated by $q\bar q \rightarrow l\bar l$, followed by $qg \rightarrow qgl\bar l$, which was an order of magnitude

lower, and $gg \to q\bar{q}l\bar{l}$ which was lower than the first process by 3 orders of magnitude [25,26]. In addition, the previous calculation of dileptons produced in thermodynamic equilibrium QGP system showed that the contributions of the gluon fusion $gg \to c\bar{c}$ and quark-antiquark annihilation $q\bar{q} \to c\bar{c}$ to dileptons strongly depended on the initial temperature of the QGP system [27].

In this work, based on Jüttner distribution function of partons, we shall study the evolution of the chemically equilibrating QGP (CEQGP) system at finite baryon density, calculate the dilepton yields from processes: quark-antiquark annihilation $q\bar{q} \to l\bar{l}$, gluon fusion $gg \to c\bar{c}$, quark-antiquark annihilation $q\bar{q} \to c\bar{c}$ and Compton-like $qg \to ql\bar{l}$, and reveal the effect of the finite baryon density on the evolution and dilepton production of the CEQGP system. The rest of the paper is organized as follows: Section II derives the thermodynamic relations and evolution equations of the system. Section III focuses on discussion of the dilepton production. In Sec. IV, we discuss the evolution of the system and calculate dilepton yields. Finally, conclusion is given in Sec. V.

II. EVOLUTION OF THE SYSTEM

A. Thermodynamic relations of the system

We first derive the thermodynamic relations of the CEQGP system at finite baryon density. Expanding densities of quarks (antiquarks),

$$n_{q(\bar{q})} = \frac{g_{q(\bar{q})}}{2\pi^2} \lambda_{q(\bar{q})} \int \frac{p^2 dp}{\lambda_{q(\bar{q})} + e^{(p \mp \mu_q)/T}}, \quad (1)$$

over the quark chemical potential μ_q, we get the baryon density of the system

$$n_{b,q} = \frac{g_q}{6\pi^2} \left[T^3(Q_1^2\lambda_q - \bar{Q}_1^2\lambda_{\bar{q}}) + 2\mu_q T^2(Q_1^1\lambda_q + \bar{Q}_1^1\lambda_{\bar{q}}) \right.$$
$$\left. + T\mu_q^2(Q_1^0\lambda_q - \bar{Q}_1^0\lambda_{\bar{q}}) + \frac{1}{3}\mu_q^3\left(\frac{\lambda_q}{\lambda_q+1} + \frac{\lambda_{\bar{q}}}{\lambda_{\bar{q}}+1}\right) \right]$$

$$(2)$$

and the corresponding energy density including the contribution of gluons,

$$\varepsilon_{QGP} = \frac{g_q}{2\pi^2}\left[T^4(Q_1^3\lambda_q + \bar{Q}_1^3\lambda_{\bar{q}}) + 3\mu_q T^3(Q_1^2\lambda_q - \bar{Q}_1^2\lambda_{\bar{q}}) \right.$$
$$+ 3\mu_q^2 T^2(Q_1^1\lambda_q + \bar{Q}_1^1\lambda_{\bar{q}}) + T\mu_q^3(Q_1^0\lambda_q - \bar{Q}_1^0\lambda_{\bar{q}})$$
$$\left. + \frac{1}{3}\mu_q^4\left(\frac{\lambda_q}{\lambda_q+1} + \frac{\lambda_{\bar{q}}}{\lambda_{\bar{q}}+1}\right) + \frac{g_g}{g_q}T^4\lambda_g G_1^3 + \frac{2\pi^2 B_0}{g_q} \right].$$

$$(3)$$

Taking $\lambda_q = \lambda_{\bar{q}} = \lambda_g = 1$, these equations become the equations of state of the thermodynamic equilibrium QGP system at finite baryon density. Where $g_{q(\bar{q})}$ and g_g are, in turn,

degeneracy factors of quarks (antiquarks) and gluons. Since the convergence of the following integral factors appearing in the expansion above

$$G_m^n = \int \frac{Z^n dZ}{(e^Z - \lambda_g)^m} \quad Q_m^n = \int \frac{Z^n dZ}{(\lambda_q + e^Z)^m}$$

$$\bar{Q}_m^n = \int \frac{Z^n dZ}{(\lambda_{\bar{q}} + e^Z)^m} \quad (4)$$

is very rapid, it is very easy to calculate these integrals, numerically.

B. Evolution equations of the system

The dominant reactions leading to chemical equilibrium are assumed to be $gg \rightleftharpoons ggg$ and $gg \rightleftharpoons q\bar{q}$. Assuming that elastic parton scatterings are sufficiently rapid to maintain local thermal equilibrium, the evolution of the parton densities can be given by the master equations. In the baryon symmetric matter which has a vanishing initial chemical potential, there is the relation $\lambda_q = \lambda_{\bar{q}}$. The calculated initial quark chemical potential for $A_u^{197} + A_u^{197}$ collisions at the RHIC energies is relatively small, as can be seen in the following calculated results and discussions based on Ref. [19]. Accordingly, for a qualitative study we take the approximation $\lambda_q = \lambda_{\bar{q}}$. Combining the master equations together with the equation of energy-momentum conservation and equation of baryon number conservation, for the longitudinal scaling expansion of the system, one can get a set of coupled relaxation equations describing evolutions of the temperature T, quark chemical potential μ_q, and fugacities λ_q for quarks and λ_g for gluons on the basis of the thermodynamic relations of the CEQGP system at finite baryon density, as obtained above,

$$\left(\frac{1}{\lambda_g} + \frac{G_2^2}{G_1^2}\right)\dot{\lambda}_g + 3\frac{\dot{T}}{T} + \frac{1}{\tau}$$
$$= R_3\left[1 - \frac{G_1^2}{2\xi(3)}\lambda_g\right] - 2R_2\left[1 - \left(\frac{2\xi(3)}{G_1^2}\right)^2 \frac{n_q n_{\bar{q}}}{\bar{n}_q \bar{n}_{\bar{q}}} \frac{1}{\lambda_g^2}\right]$$

$$(5)$$

$$\dot{\lambda}_q\left[T^3(Q_1^2 - \lambda_q Q_2^2) + 2\mu_q T^2(Q_1^1 - \lambda_q Q_2^1)\right.$$
$$\left. + T\mu_q^2(Q_1^0 - \lambda_q Q_2^0) + \frac{1}{3}\mu_q^3\frac{1}{(\lambda_q+1)^2}\right]$$
$$+ \dot{T}[3\lambda_q T^2 Q_1^2 + 4\lambda_q \mu_q T Q_1^1 + \lambda_q \mu_q^2 Q_1^0]$$
$$+ \dot{\mu}_q\left[2\lambda_q T^2 Q_1^1 + 2\lambda_q \mu_q T Q_1^0 + \mu_q^2\frac{\lambda_q}{(\lambda_q+1)}\right] + \frac{n_q^0}{\tau}$$
$$= n_g^0 R_2\left[1 - \left(\frac{2\xi(3)}{G_1^2}\right)^2 \frac{n_q n_{\bar{q}}}{\bar{n}_q \bar{n}_{\bar{q}}} \frac{1}{\lambda_g^2}\right]$$

$$(6)$$

$$\dot\lambda_q\left[4\mu_qT^2(Q_1^1-\lambda_qQ_1^1)+\frac{2}{3}\mu_q^3\frac{1}{(\lambda_q+1)^2}\right]$$

$$+\dot T8\mu_qTQ_1^1\lambda_q+\dot\mu_q\left[4T^2Q_1^1\lambda_q+2\mu_q^2\frac{\lambda_q}{(\lambda_q+1)}\right]$$

$$=-\frac{1}{\tau}\left[4\mu_qT^2Q_1^1\lambda_q+\frac{2}{3}\mu_q^3\frac{\lambda_q}{\lambda_q+1}\right]\qquad(7)$$

$$\dot\lambda_g\frac{g_g}{g_q}T^4(G_1^3+\lambda_gG_2^3)+\dot\lambda_q\left[2T^4(Q_1^3-\lambda_qQ_2^3)\right.$$

$$\left.+6T^2\mu_q^2(Q_1^1-\lambda_qQ_2^1)+\frac{2}{4}\mu_q^4\frac{1}{(\lambda_q+1)^2}\right]$$

$$+\dot T\left[8T^3Q_1^3\lambda_q+12\mu_q^2TQ_1^1\lambda_q+4\frac{g_g}{g_q}T^3\lambda_gG_1^3\right]$$

$$+\dot\mu_q\left[12\mu_qT^2Q_1^1\lambda_q+2\mu_q^3\frac{\lambda_q}{\lambda_q+1}\right]$$

$$=-\frac{1}{\tau}\left[2T^4Q_1^3\lambda_q+6\mu_q^2T^2Q_1^1\lambda_q\left(\frac{\lambda_{\bar q}}{\lambda_{\bar q}+1}\right)\right.$$

$$\left.+\frac{g_g}{g_q}T^4\lambda_gG_1^3+\frac{2\pi B_0}{g_q}\right],\qquad(8)$$

where $\bar n_{q(\bar q)}$ is the value of $n_{q(\bar q)}$ at $\lambda_{q(\bar q)}=1$, $n_q^0=n_q/(g_q/2\pi^2)$, $n_g^0=n_g/(g_g/2\pi^2)$, the bag constant $B_0^{1/4}=250$ MeV, and $\xi(3)=1.202\,06$. The gluon and quark production rates R_3/T and R_2/T are, in turn, given by

$$R_3/T=\frac{32}{3a_1}\frac{\alpha_s}{\lambda_g}\left[\frac{(M_D^2+s/4)M_D^2}{9g^2T^4/2}\right]^2I(\lambda_g,\lambda_q,T,\mu_q),\quad(9)$$

$$R_2/T=\frac{g_g}{24\pi}\frac{G_1^{12}}{G_1^2}N_f\alpha_s^2\lambda_g\ln(1.65/\alpha_s\lambda),\qquad(10)$$

$$M_D^2=\frac{3g^2T^2}{\pi^2}\left[2G_1^1\lambda_g+2N_fQ_1^1\lambda_q+\left(\frac{\mu_q}{T}\right)^2\left(\frac{\lambda_q}{\lambda_q+1}\right)\right],\qquad(11)$$

where M_D^2 is the Debye screening mass, $a_1=g_gG_1^2/2\pi^2$, $g^2=4\pi\alpha_s$, and $I(\lambda_g,\lambda_q,T,\mu_q)$ is the function of λ_g, λ_q, T, μ_q. We here take the quark flavor $N_f=2.5$ as done [17,18,22].

III. DILEPTON PRODUCTION

With the given evolution of the parton system, one can calculate lepton pairs created through quark-antiquark annihilation $q\bar q\to l\bar l$ and thermal charmed quark decays during the equilibration of the system. With a high initial temperature in the most optimistic scenario, $T_{i,max}\approx(\frac{1}{3}-\frac{1}{2})m_c$, a significant thermal charm production may be expected [27–29], where m_c is the mass of the charmed quark. For the QGP system, produced in collisions at the RHIC energies, with very high initial temperature (~0.57 GeV) [17], ther-

mal charmed quark productions and their contributions to lepton pairs should be included. Especially, those from the gluon fusion $gg\to c\bar c$ and quark-antiquark annihilation $q\bar q\to c\bar c$ are important. We now compute the rate of lepton pair production from the quark-antiquark annihilation $q\bar q\to l\bar l$. According to the discussion in Ref. [30], the number of produced pairs in a space-time volume element d^4x and of invariant mass M can be expressed by the elementary formula

$$\frac{dN}{d^4xdM^2}=\int d^4p_1d^4p_2\delta(p_1^2)\delta(p_2^2)p_{01}p_{02}\theta(p_{01})\theta(p_{02})Q_q^2v$$

$$\times\sigma(M)f_q(p_{01})f_{\bar q}(p_{02})\delta(M^2-(p_1+p_2)^2),\quad(12)$$

where $f_{q(\bar q)}$ stand for the Jüttner distribution function of quarks (antiquarks), Q_q the charge, v the relative velocity of the annihilating quark pair. The quark annihilation cross section $\sigma(M)$ into leptons of mass m_l is generally given by [4,5,8,10,25,30]

$$\sigma(M)=\frac{4\pi\alpha^2}{M^2}\left(1+\frac{2m_l^2}{M^2}\right)\left(1-\frac{4m_l^2}{M^2}\right)^{1/2},\qquad(13)$$

where α is the fine-structure constant. For the quark flavor $N_f=2.5$, we obtain the expression as

$$\frac{dN}{d^4xdM^2}$$

$$=\frac{8}{3}\frac{M^2}{(2\pi)^4}\lambda_q^2\int\frac{dp_{01}dp_{02}\sigma(M)\theta(4p_{01}p_{02}-M^2)}{[e^{(p_{01}-\mu_q)/T}+\lambda_q][e^{(p_{02}+\mu_q)/T}+\lambda_q]}.$$

$$(14)$$

Introducing the substitution $p_{01}/T=x$, $p_{02}/T=y$, $\mu_q/T=z$, and $M/T=u$, for the longitudinal scaling expansion, we finally have

$$\frac{dN}{dM^2dY}$$

$$=\frac{8}{3}\frac{M^2}{(2\pi)^4}\pi R^2\int\lambda_q^2\frac{dxdyd\tau\tau T^2\sigma(M)\theta(xy-u^2/4)}{[e^{x-z}+\lambda_q][e^{y+z}+\lambda_q]}.$$

$$(15)$$

Since these integrals are numerically performed, we can obtain more accurate results. The degeneracy factors for quarks and gluons are, respectively, $g_q=N_f(2\times3)$ and $g_g=(2\times8)/2$ (the factor of 1/2 is needed to prevent double counting), the cross sections for reactions $q\bar q\to c\bar c$ and $gg\to c\bar c$ in leading-order QCD have been given in Refs. [27,29,31]. Therefore, similar to the calculation for $q\bar q\to l\bar l$, we can obtain the yields of reactions $q\bar q\to c\bar c$ and $g\bar g\to c\bar c$. Almost, all of the produced thermal charmed quarks would eventually hadronize to D mesons [27]. Considering that the D meson decays to leptons with a 34% branching ratio (or either a μ or an e) for charged D mesons, or a 15% branching ratio for neutral D mesons [27,32], finally one can get the contribution of charmed quarks from reactions $q\bar q\to c\bar c$ and $gg\to c\bar c$ to lepton pairs. Also here, we neglect charm fragmen-
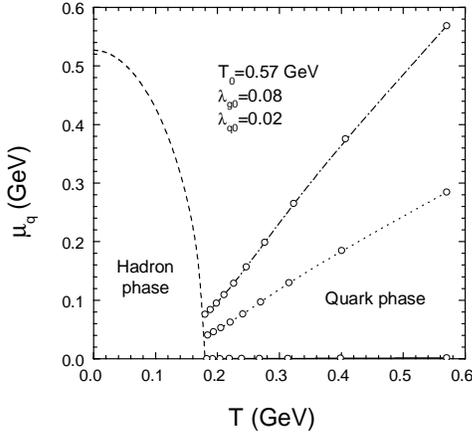
FIG. 1. The calculated evolution paths of the system in phase diagram for initial values $\tau_0 = 0.70$ fm, $T_0 = 0.57$ GeV, $\lambda_{g0} = 0.08$, and $\lambda_{q0} = 0.02$, where the solid, dotted, and dash-dotted lines are, in turn, the calculated paths for initial quark chemical potentials $\mu_{q0} = 0.000$, 0.284, and 0.568 GeV. The time interval between the two small circles is 0.5 fm (i.e., $50 \times$ calculation-step 0.01 fm). The phase diagram is calculated at $B^{1/4} = 0.250$ GeV, where the phase boundary is denoted by the dashed line.

tation [27,28]. Finally, we also calculate the contribution of the Compton-like reaction $qg \rightarrow ql\bar{l}$ to dileptons.

IV. CALCULATED RESULTS AND DISCUSSIONS

In this work we focus on discussing $A_u^{197} + A_u^{197}$ collisions at the RHIC energies. Hammon *et al.* [19] have calculated the nonequilibrium initial conditions from the perturbative QCD within the Glauber multiple scattering theory for $\sqrt{s} = 200A$ GeV and $\sqrt{s} = 5.5A$ TeV. Taking into account higher order contribution by a K-factor 2.5 at the RHIC experiment [33], they have obtained the energy density and number densities of gluons, quarks, and antiquarks as well as the initial temperature $T_0 = 0.552$ GeV. From these densities we have also obtained initial temperature $T_0 = 0.566$ GeV and initial quark chemical potential $\mu_{q0} = 0.284$ GeV, based on thermodynamic relations of the CEQGP system with finite baryon density, as mentioned in the preceding part, at $\lambda_{g0} = 0.08$ and $\lambda_{q0} = 0.02$. Obviously, these initial temperatures are near the one from Hijing model calculation in Ref. [17]. With the help of the results of the Hijing model, we take the initial values of the system: $\tau_0 = 0.70$ fm, $T_0 = 0.57$ GeV, $\lambda_{g0} = 0.08$, and $\lambda_{q0} = 0.02$. To further understand the effect of the finite baryon density on dilepton yields, we extend our calculation up to the initial quark chemical potential $\mu_{q0} = 0.568$ GeV. We have solved the set of coupled relaxation equations (5)–(8) for initial quark chemical potentials $\mu_{q0} = 0.000$, 0.284, and 0.568 GeV, and obtained the evolutions of the temperature, quark chemical potential, and fugacities λ_g and λ_q of the system. The calculated evolution paths of the system in the phase diagram have been shown in Fig. 1, where the solid, dotted, and dash-dotted lines are, in turn, the evolution paths for initial quark chemical potentials $\mu_{q0} = 0.000$, 0.284, and 0.568 GeV at $T_0 = 0.57$ GeV, and the dashed line is the phase boundary of the phase diagram.
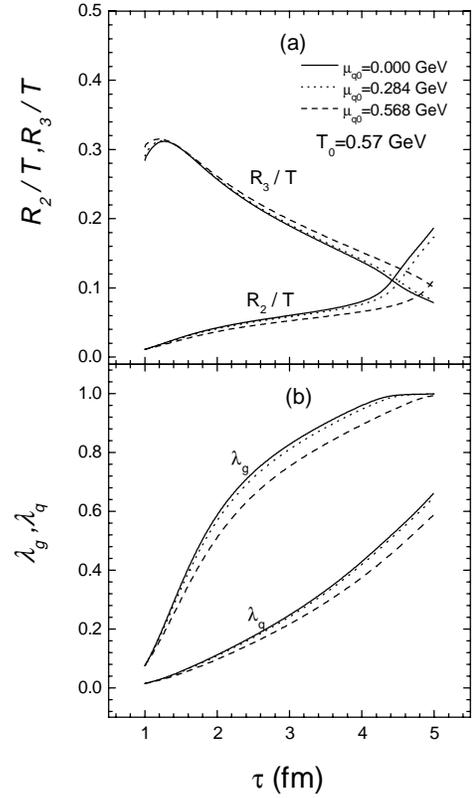
FIG. 2. The calculated parton production rates R_2/T for quarks and R_3/T for gluons in panel (a), and fugacities λ_q for quarks and λ_g for gluons in panel (b) under the same initial conditions as given in Fig. 1. The solid, dotted, and dashed lines in these two panels denote, in turn, the calculated values for initial quark chemical potentials $\mu_{q0} = 0.000$, 0.284, and 0.568 GeV.

While in order to give a deeper insight into the dynamical evolution of the QGP, we have marked the equal time step on the paths in Fig. 1. The time interval between the two small circles is 0.5 fm (i.e., $50 \times$ calculation-step 0.01 fm). We can see from Fig. 1 that the evolution of the system becomes slower and slower with the increase of the evolution time. The calculated parton production rates R_2/T for quarks and R_3/T for gluons, and fugacities λ_q for quarks and λ_g for gluons are, in turn, shown in (a) and (b) panels of Fig. 2. The solid, dotted, and dashed lines in every panel of Fig. 2 denotes, respectively, the values for initial quark chemical potentials $\mu_{q0} = 0.000$, 0.284 and 0.568 GeV. In this work, due to adopting Jüttner distribution as the phase space distribution function of partons, the Debye screening mass M_D^2 changes with the quark chemical potential as seen in Eq. (11). According to Eq. (9) the gluon production rate R_3/T rapidly goes down with the evolution time as shown in panel (a). Thus, the chemical equilibration rate of the system necessarily goes up rapidly with evolution time, the fugacities of gluons and quarks can, respectively, reach the equilibrium values by evolution times $\tau \approx 4.36$ fm (where the temperature drops to about 150 MeV) and 7.12 fm, as shown in panel (b)2. The similar characters have been seen in chemically equilibrating baryon-free QGP [24], where the gluon

chemical equilibration rate is heightened through taking large parameter Λ.

We now discuss the effect of the finite initial quark chemical potential on the evolution of the system. We know that the baryon-free QGP converts into the hadronic matter, only with decreasing temperature along the temperature axis of the phase diagram, and the phase transition occurs at a certain critical temperature T_c. However, in this work, both the quark chemical potential and the temperature of the system are functions of time, compared with the baryon-free QGP, it necessarily takes a long time for value (μ_q, T) of the system to reach a certain point of the phase boundary between the quark phase and the hadronic phase to make the phase transition. Such an effect will cause the increase of the lifetime of the quark phase. Furthermore, we have found that with increasing initial quark chemical potential, the production rate R_3/T of gluons goes up as shown in panel (a) of Fig. 2. Thus the gluon equilibration rate goes down as seen in panel (b) of Fig. 2, leading to the low energy consumption of the system, i.e., slow cooling of the system. Since gluons are much more than quarks in the CEQGP system, overall with increasing initial quark chemical potential, the cooling of the system slows down. Therefore, the quark phase lifetime further increases. One can see in Fig. 1 that the increase of the initial quark chemical potential μ_{q0} will change the hydrodynamic behavior of the CEQGP system with finite baryon density to cause the increase of the quark phase lifetime. The calculated presence times of the system in the quark phase for initial quark chemical potentials $\mu_{q0}=0.000$, 0.284, and 0.568 GeV are, in turn, 4.19, 4.52, and 4.87 fm.

We have calculated dilepton spectra dN/dM^2dY from $q\bar{q}\to l\bar{l}$ annihilation, as shown in panel (a) of Fig. 3. The dotted, solid, and dashed lines are, in turn, the spectra for initial quark chemical potentials $\mu_{q0}=0.000$, 0.284, and 0.568 GeV at the initial temperature $T_0=0.57$ GeV. It is well known that in the thermodynamic equilibrium QGP system, the dilepton yield from $q\bar{q}\to l\bar{l}$ annihilation is suppressed with increasing initial quark chemical potential μ_{q0} [9,11,24]. However, as pointed out in the discussions in the above section, with increasing initial quark chemical potential μ_{q0}, the quark phase lifetime will increase. Accordingly, the contribution of the quark phase to dileptons is heightened. For the QGP system, produced at the RHIC energies, with high initial temperature, this effect becomes even more significant. Therefore, one can see from the dotted, solid, and dashed lines in panel (a) that in the CEQGP system, the dilepton yield will go up with increasing initial quark chemical potential. Compared with the calculated dilepton yield in the thermodynamic equilibrium QGP system, where the dilepton yield is suppressed with the increase of the initial quark chemical potential, this enhancement of the yield is important. In panel (b), we also show the calculated dilepton spectra dN/dM^2dY from $q\bar{q}\to l\bar{l}$ annihilation at a lower initial temperature $T=0.238$ GeV under the same conditions as given in panel (a). The calculated dilepton spectrum is still an increasing function of the initial quark chemical potential. It shows that the increasing effect of the quark phase lifetime with increasing initial quark chemical potential μ_{q0} is essen-
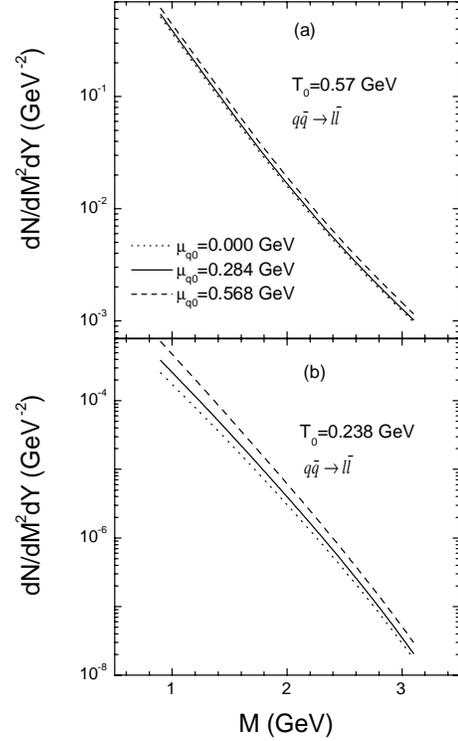
FIG. 3. The calculated dilepton spectra dN/dM^2dY from reaction $q\bar{q}\to l\bar{l}$. The dotted, solid, and dashed lines in panel (a) are, in turn, the calculated spectra for initial quark chemical potentials $\mu_{q0}=0.000$, 0.284, and 0.568 GeV under the same initial conditions as given in Fig. 1. In panel (b), the initial temperature T_0 is taken as 0.238 GeV.

tially governed by the characteristic evolution behavior of the CEQGP system with finite baryon density.

In order to further understand the relation between the dilepton production in the CEQGP system and the initial quark chemical potential μ_{q0}, we have calculated the integrated yield dN/dY for the reaction $q\bar{q}\to l\bar{l}$ within the time region from τ_0 to τ, which, as a function of the initial quark chemical potential μ_{q0}, is shown in Fig. 4. The dash-dotted, dotted, dashed, and solid lines represent, in turn, the integrated yields at the evolution times $\tau=2.0$, 2.5, 3.0, and 3.5 fm for $T_0=0.57$ GeV. In initial stage, since the increasing effect of the quark phase lifetime with increase of the initial quark chemical potential μ_{q0} is not obvious, the increase of the yield is smaller. However, with further increasing evolution time τ, the increasing effect of the QGP lifetime becomes important and can even compensate the suppression. Thus, the calculated yield goes up with the increase of the initial quark chemical potential μ_{q0}, as seen in Fig. 4. It further shows that the dilepton yield in the CEQGP system with finite baryon density is no longer a monotonically decreasing function of the initial quark chemical potential.

In Fig. 5, we show the calculated dilepton spectra dN/dM^2dY from processes: fusion $gg\to c\bar{c}$, annihilation $q\bar{q}\to c\bar{c}$, annihilation $q\bar{q}\to l\bar{l}$, the Compton-like reaction $qg\to ql\bar{l}$, and their total, which are, in turn, represented by the dashed, short-dashed, dash-dotted, dotted, and solid lines.
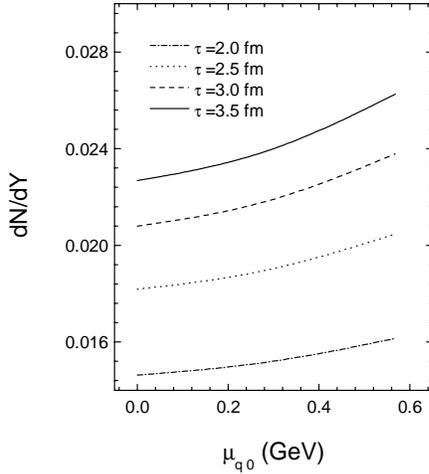
FIG. 4. The calculated integrated yields dN/dY as function of the initial quark chemical potential μ_{q0} for given evolution times τ. The dash-dotted, dotted, dashed, and solid lines are, in turn, the integrated yields at evolution times $\tau = 2.0$, 2.5, 3.0, and 3.5 fm under the same initial conditions as given in Fig. 1.

Due to strong dependence of the gluon fusion ($gg \rightarrow c\bar{c}$) and quark-antiquark annihilation ($q\bar{q} \rightarrow c\bar{c}$) yields on the initial temperature, and other factors, such as, larger cross section of the fusion reaction $gg \rightarrow c\bar{c}$ in the intermediate mass region [27] as well as larger gluon density in the CEQGP system, thermal charmed quarks from $gg \rightarrow c\bar{c}$ and $q\bar{q} \rightarrow c\bar{c}$ reactions, provide important contributions to dileptons during the evolution, as seen from the dash-dotted, dotted lines in Fig. 5, leading to the enhancement of dileptons with intermediate masses, as seen from the solid line in Fig. 5. The calculated spectrum is found to be dominated by the fusion $gg \rightarrow c\bar{c}$, followed by the annihilation $q\bar{q} \rightarrow c\bar{c}$ which is half
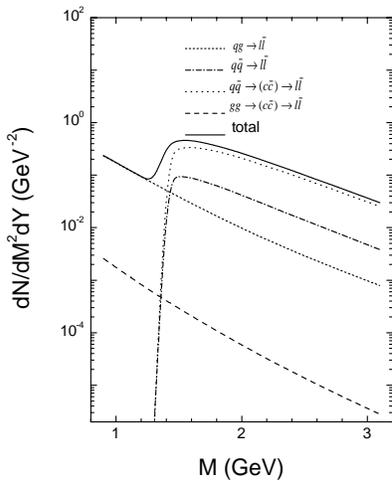
FIG. 5. The calculated dilepton spectra dN/dM^2dY at the initial quark chemical potential $\mu_{q0} = 0.284$ GeV under the same initial conditions are as given in Fig. 1. The dashed, short-dashed, dash-dotted, dotted and solid lines denote, in turn, the calculated spectra from the Compton-like reaction $qg \rightarrow ql\bar{l}$, annihilation $q\bar{q} \rightarrow l\bar{l}$, fusion $gg \rightarrow c\bar{c}$, annihilation $q\bar{q} \rightarrow c\bar{c}$ and their total.
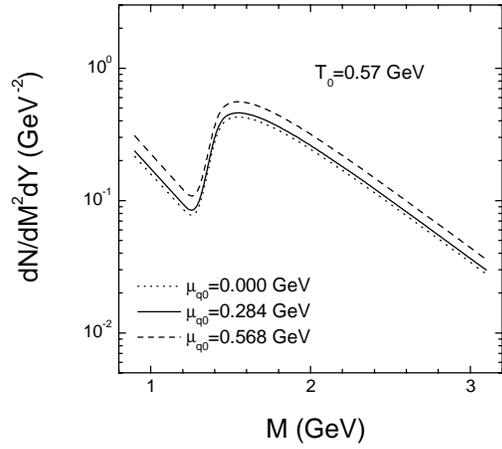
FIG. 6. The calculated total dilepton yields dN/dM^2dY (of processes: the Compton-like reaction $qg \rightarrow ql\bar{l}$, annihilation $q\bar{q} \rightarrow l\bar{l}$, fusion $gg \rightarrow c\bar{c}$, and annihilation $q\bar{q} \rightarrow c\bar{c}$) under the same initial conditions as given in Fig. 1. The dotted, solid and dashed lines represent, in turn, the total yields for initial quark chemical potentials $\mu_{q0} = 0.000$, 0.284, and 0.568 GeV.

an order of magnitude lower, the contribution of the annihilation $q\bar{q} \rightarrow l\bar{l}$, which is lower than the one of the first processes by 2 orders of magnitude, and the contribution of the Compton-like reaction $qg \rightarrow ql\bar{l}$, which is lower than that of the third process by about 2 orders of magnitude. In addition, in Fig. 6, we have shown total yields (of those 4 reactions mentioned above) for initial quark chemical potentials $\mu_q = 0.000$, 0.284, and 0.568 GeV at $T_0 = 0.57$ GeV, which are denoted by dotted, solid, and dashed lines, respectively. It also shows clearly that the dilepton yield from $q\bar{q} \rightarrow l\bar{l}$ in the CEQGP system with finite baryon density is an increasing function of the initial quark chemical potential. Adding the contribution from reactions $gg \rightarrow c\bar{c}$ and $q\bar{q} \rightarrow c\bar{c}$, one can obtain the significantly enhanced dileptons with intermediate masses.

V. CONCLUSION

In this work, in order to study the dilepton production in a chemically equilibrating QGP system with finite baryon density, based on the Jüttner distribution function of partons, we have derived a set of coupled relaxation equations from the conservation laws of the energy-momentum and baryon number, considering that the dominant reactions leading to chemical equilibrium are the processes $gg \rightleftharpoons ggg$ and $gg \rightleftharpoons q\bar{q}$. We have also obtained the expression of dilepton production under the same conditions. Subsequently, we have studied the evolution and dilepton yields of the system produced from $A_u^{197} + A_u^{197}$ collisions at the RHIC energies. We have found that the increase of the initial quark chemical potential μ_{q0} will change the hydrodynamic behavior of the CEQGP system to cause the increase of the quark phase lifetime. First, this effect is to heighten the dilepton yield from the reaction $q\bar{q} \rightarrow l\bar{l}$ and compensate and even surpass the dilepton suppression effect caused by the increase of the

initial quark chemical potential, making the dilepton yield as an increasing function of the initial quark chemical potential. On the other hand, we should stress that the increase of the quark phase lifetime also heightens the thermal charmed quark production to make the contribution of thermal charmed quarks to dilepton further go up. Especially, due to higher initial temperature, larger gluon density of the system as well as larger reaction cross sections of $gg \rightarrow c\bar{c}$ and $q\bar{q} \rightarrow c\bar{c}$ in the intermediate mass region, thermal charmed quarks from the fusion $gg \rightarrow c\bar{c}$ and annihilation $q\bar{q} \rightarrow c\bar{c}$ can provide a dominant contribution to dileptons at intermediate masses, leading to a further increase of the dilepton yield. Therefore, in a CEQGP system with finite baryon density created at the RHIC energies, one might observe the significant enhancement of dileptons with intermediate masses.

In this work, we have studied the evolution of the CEQGP with finite baryon density based on the longitudinal scaling expansion model, neglecting the effect of the nonhomogeneous distribution of the particle in space, higher order gluon processes and temperature dependence of the strong coupling constant α_s. In the dilepton calculation, we have taken $\alpha_s = 0.3$, $m_c = 1.2$ GeV, and $K = 2.5$ to include contribution from next-to-leading order, as done in the calculation in the chemically equilibrating baryon-free QGP.

[1] T. Matsui and H. Satz, Phys. Lett. B **178**, 416 (1986).
[2] J. Rafelski and B. Müller, Phys. Rev. Lett. **48**, 1066 (1982).
[3] E. Shuryak, Phys. Rep. **80**, 71 (1980).
[4] K. Kajantie, J. Kapusta, L. McLerran, and A. Mekjian, Phys. Rev. D **34**, 2746 (1986).
[5] A. Dumitru *et al.*, Phys. Rev. Lett. **70**, 2860 (1993).
[6] J.D. Bjorken, Phys. Rev. D **27**, 140 (1983).
[7] K. Kajantie, J. Kapusta, and A. Mekjian, Phys. Rev. D **34**, 2746 (1986).
[8] L.H. Xia, C.M. Ko, and C.T. Li, Phys. Rev. C **41**, 572 (1990).
[9] J. Sollfrank *et al.*, Phys. Rev. C **55**, 392 (1997).
[10] Z.J. He, J.J. Zhang, X.J. Qiu, and J.F. Chen, Nucl. Phys. **A614**, 552 (1997).
[11] Z.J. He *et al.*, Phys. Lett. B **495**, 317 (2000).
[12] E. Shuryak, Phys. Rev. Lett. **68**, 3270 (1992).
[13] K.J. Eskola and X.N. Wang, Phys. Rev. D **49**, 1284 (1994).
[14] D.K. Srivastava, M.G. Mustafa, and B. Müller, Phys. Lett. B **396**, 451 (1997).
[15] K. Geiger, Phys. Rev. D **48**, 4129 (1993).
[16] E. Shuryak and L. Xiong, Phys. Rev. Lett. **70**, 2241 (1993).
[17] T.S. Biró *et al.*, Phys. Rev. C **48**, 1275 (1993).
[18] C.T. Traxler and M.H. Thoma, Phys. Rev. C **53**, 1345 (1996).
[19] N. Hammon, H. Stöker, and W. Greiner, Phys. Rev. C **61**, 014901 (1999).
[20] K. Geiger and J.I. Kapusta, Phys. Rev. D **47**, 4905 (1993).
[21] A. Majumder and C. Gale, Phys. Rev. D **63**, 114008 (2001).
[22] P. Levai, B. Müller, and X.N. Wang, Phys. Rev. C **51**, 3326 (1995).
[23] T. Matsui, B. Svetitsky, and L. McLerran, Phys. Rev. D **34**, 783 (1986).
[24] B. Kämpfer *et al.*, Z. Phys. A **353**, 71 (1995).
[25] B. Kämpfer, O.P. Pavlenko, A. Peshier, and G. Soff, Phys. Rev. C **52**, 2704 (1995).
[26] Z. Lin and C.M. Ko, Nucl. Phys. **A671**, 567 (2000).
[27] A. Shor, Phys. Lett. B **215**, 375 (1988); **233**, 231 (1989); B.L. Combridge, Nucl. Phys. **B151**, 429 (1979).
[28] R. Vogt, B.V. Jacak, P.L. McGaughey, and P.V. Ruuskanen, Phys. Rev. D **49**, 3345 (1994).
[29] S. Gavin, P.L. McGaughey, P.V. Ruuskanen, and R. Vogt, Phys. Rev. C **54**, 2606 (1996).
[30] G. Domokos and J.I. Goldman, Phys. Rev. D **23**, 203 (1981).
[31] J.O. Schmitt, G.C. Nayak, H. Stöcker, and W. Greiner, Phys. Lett. B **498**, 163 (2001).
[32] R.M. Baltrusaitis *et al.*, Phys. Rev. Lett. **54**, 1976 (1985).
[33] K.J. Eskola, K. Kajantie, and J. Lindfors, Nucl. Phys. **B323**, 37 (1989); C. Albaja *et al.*, UA1 Collaboration, *ibid.* **B309**, 405 (1988).